# Effect of Optical Coherence Tomography Scan Pattern and Density on the Detection of Full-Thickness Macular Holes

ERIC W. SCHNEIDER, BOZHO TODORICH, MICHAEL P. KELLY, AND TAMER H. MAHMOUD

• PURPOSE: **To evaluate the impact of different scan patterns and scan densities on small full-thickness macular hole (MH) detection.**

• DESIGN: **Retrospective cross-sectional analysis.**

• METHODS: **Analysis was performed on 25 eyes from 24 patients with full-thickness MHs imaged with the Heidelberg Spectralis HRA+OCT. Included eyes underwent concurrent imaging with a standard (61-line) raster volume and a 24-line radial pattern. A 6-line radial scan pattern was extrapolated from the higher-density radial pattern. Comparisons of the missed hole rate as well as the proportion of individual B-scans demonstrating a full-thickness defect (termed "full-thickness detection index") were carried out for the 3 scan patterns. Additionally, qualitative and quantitative hole parameters were evaluated to identify factors associated with "missed" holes.**

• RESULTS: **Full-thickness defects were missed at substantially higher rates using both standard raster volume (20.0%, 90% confidence interval [CI] 8.2%–37.5%) and 6-line radial scanning (12.0%, 90% CI 3.7%–30.4%) when compared to 24-line radial scanning (0% for both comparisons). Full-thickness detection indices were significantly higher for both radial scan patterns when compared to raster scanning ($P < .001$ for both comparisons). Missed holes were smaller and commonly associated with prehole flaps.**

• CONCLUSION: **High-density radial scanning demonstrated superior detection rates of small full-thickness MHs compared to standard raster volume scanning. This finding may be attributable to the greater foveolar scan density attained with radial scan patterns. Failure to utilize radial scanning in the setting of suspected macular holes may lead to a delay in surgical treatment, with attendant worse anatomic and visual outcomes. (Am J Ophthalmol 2014;157:978–984. © 2014 by Elsevier Inc. All rights reserved.)**

WITH MODERN VITREORETINAL TECHNIQUES, including internal limiting membrane peeling, reported anatomic closure rates for full-thickness macular holes (MH) are routinely greater than 95%.[1–3] Regression analyses have identified several factors associated with higher closure rates and better visual outcomes, including lower hole stage, smaller hole diameter, and shorter duration of symptoms.[4–6] As natural history studies of stage 2 holes have demonstrated high rates of hole enlargement with progression to stage 3-4 without treatment,[7] earlier surgical repair would potentially result in better anatomic and visual outcomes.

Maximizing diagnostic sensitivity thus becomes important as it allows for the detection of smaller/earlier macular holes. Currently, optical coherence tomography (OCT) provides detailed in vivo visualization of foveal integrity and the vitreoretinal interface far superior to that achievable with slit-lamp biomicroscopy, particularly for smaller holes.[8] In theory, OCT-assisted diagnosis of macular holes may thus provide for more timely diagnosis and treatment of smaller/earlier full-thickness MHs with attendant better postoperative outcomes.

Diagnostic sensitivity for macular hole detection may be further improved via the design of OCT scanning protocols with B-scan pattern and density optimized for the detection of foveal pathology. Recent work has focused on the impact of OCT scan density on the detection of qualitative features of neovascular age-related macular degeneration (AMD)[9] as well as on the accuracy of retinal thickness measurements in diabetic macular edema (DME).[10] While these studies did demonstrate numerically inferior results with lower scan densities, the authors were careful to highlight that the sensitivity/accuracy of OCT assessments was clinically acceptable at B-scan densities one-quarter to one-eighth as high as those provided by the standard 128 B-scan/6 mm macular cube (Cirrus HD-OCT, Carl Zeiss Meditec; 3D OCT-1000, Topcon).[9,10] This would seem to indicate a lesser importance for OCT scan density in optimizing scan protocols for neovascular AMD and DME.

Unlike neovascular AMD and DME, however, the pathologic features in idiopathic macular holes are by definition located at the foveal center. As such, the typical raster-based macular volume scan protocols—designed for evaluation of the more widespread macular pathology seen in neovascular AMD and DME—may be poorly suited for sensitive detection of small full-thickness MHs. Moreover, clinically important characteristics of idiopathic macular holes, such as the presence of a small inner retinal opening, are typically focal and often exceedingly small. B-scan density may thus have a greater impact on the sensitivity of full-thickness MH detection as compared to detection of

AJO.com Supplemental Material available at AJO.com.
Accepted for publication Jan 22, 2014.

From Duke University Eye Center, Department of Ophthalmology, Duke University, Durham, North Carolina.

Inquiries to Dr Tamer H. Mahmoud, Duke University Eye Center – Vitreoretinal Surgery, 2351 Erwin Road DUMC 3802, Durham, NC 27710; e-mail: tamer.mahmoud@dm.duke.edu



0002-9394/$36.00
http://dx.doi.org/10.1016/j.ajo.2014.01.021

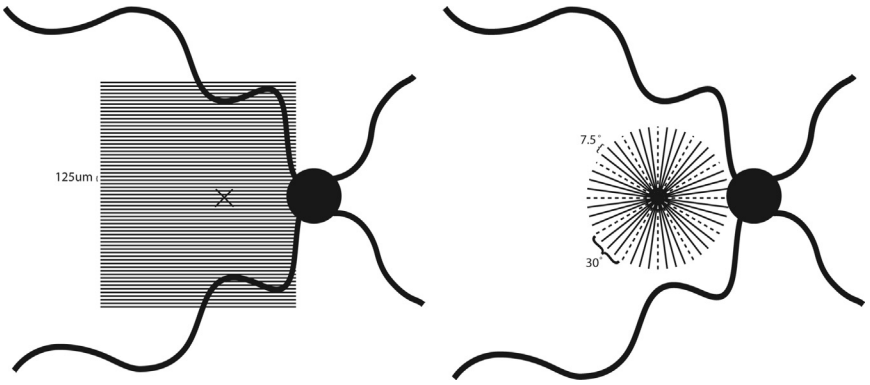


**FIGURE 1. Schematic detailing investigational optical coherence tomography scan patterns used in this study. (Left) The standard raster volume scan pattern used by the Duke Eye Center Imaging Unit is composed of 61 horizontally oriented raster B-scans (8.2 mm in length) with 125 μm interscan spacing. (Right) The historic 6-line radial scan (dashed lines only) is composed of 6 radial B-scans (5.5 mm in length) centered at the fovea with 30 degrees interscan spacing while the 24-line radial scan (dashed and solid lines) is composed of 24 radial B-scans (5.5 mm in length) centered at the fovea with 7.5 degrees interscan spacing.**

more macroscopic features (eg, subretinal fluid, pigment epithelial detachments) associated with neovascular AMD.

In this report, we use a retrospective cross-sectional design to examine the effect of different OCT scan patterns (raster vs radial) and scan densities on the detection of full-thickness defects in a cohort of small full-thickness MHs.

## MATERIALS AND METHODS

THIS WAS A RETROSPECTIVE, CROSS-SECTIONAL ANALYSIS in which clinical data and OCT images were reviewed for patients diagnosed with a macular hole based on receipt of International Classification of Diseases (9th revision) code 362.54 as identified by billing records. This study was prospectively approved by the Duke University Institutional Review Board and adhered to the tenets set forth in the Declaration of Helsinki.

Beginning in March 2012, the Duke University Eye Imaging Center adopted a policy in which patients with suspected small macular holes underwent evaluation with concurrent 24-line radial scanning (24 B-scans with 7.5 degrees interscan spacing) in addition to the Duke Eye Center Imaging Unit standard raster volume scan (61 B-scans with 125 μm interscan spacing) using the Heidelberg Spectralis OCT unit (Heidelberg Engineering, Heidelberg, Germany) (Figure 1). This allowed for the performance of a retrospective cross-sectional analysis comparing the relative rates of full-thickness MH (FTMH) detection using different scan patterns (radial vs raster) and scan densities (24-line radial vs 6-line radial). Of note, the 6-line radial scan pattern was not acquired independently, but rather was extrapolated from the 24-line radial scan based on the standard location of the 6 B-scans comprising this pattern. Ophthalmic photographers were instructed to manually center both scan patterns on the foveola if eccentric fixation was detected during OCT acquisition.

In order to be included in the analysis, patients had to have undergone concurrent raster volume and 24-line radial scanning between March 1, 2012, and October 31, 2012, and have evidence of a full-thickness MH on ≥1 B-scan on either scan pattern. Exclusion criteria included prior vitreoretinal surgery, pathologic myopia, and a history of neovascular AMD, proliferative diabetic retinopathy, solar retinopathy, or significant ocular trauma. The primary outcome was missed hole rate, which is calculated as follows (for comparison of scan pattern A to scan pattern B):

$$\textit{Missed hole rate}_{\text{A vs B}} = \frac{\textit{n without FTMH on scan pattern A}}{\textit{n with FTMH on scan pattern A or B}} \times 100$$

Secondary outcomes included a full-thickness detection index for each scan pattern/density, a derived proportion equal to the number of B-scans in a single study depicting a full-thickness defect divided by the number of B-scans depicting any outer retinal defect (with or without an associated full-thickness component). Additionally, various qualitative and quantitative hole parameters were analyzed for possible statistical associations with the occurrence of a "missed" hole using specific scan patterns/densities. Figure 2 details the characteristics/parameters assayed. All parameters were manually assessed by 2 independent masked graders (E.S., B.T.) using the Heidelberg Heyex viewing module.

Statistical analysis was carried out using SPSS Statistics, v 20.0 (IBM, Armonk, New York, USA). Categorical variables were reported as proportions and continuous variables as median ± standard deviation (SD). Exact confidence intervals (Clopper-Pearson) were calculated for missed hole rate proportions. Exact nonparametric tests were used for comparisons of full-thickness detection indices and largest/smallest minimum linear hole diameters between different scan patterns/densities (Wilcoxon signed rank test) as well as for comparisons of quantitative hole

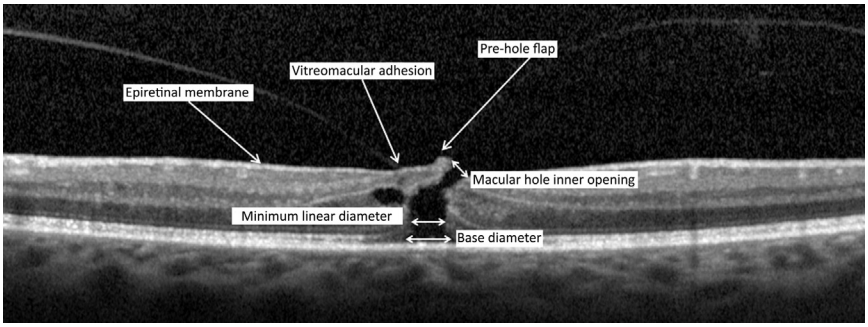


**FIGURE 2. Spectral-domain optical coherence tomography image detailing the various qualitative and quantitative parameters assessed in this study. Quantitative parameters were composed of macular hole diameters measured at different levels within the retina: at the retinal surface (macular hole inner opening), at the narrowest point within the hole (minimum linear diameter), and at the retinal pigment epithelium (RPE) (base diameter). The latter 2 measures were defined by lines parallel to the RPE. The macular hole inner opening was measured only in eyes with a prehole flap and was defined as the minimum distance from the inner flap edge to the retinal surface.**

**TABLE 1.** Impact of Optical Coherence Tomography Scan Pattern on Full-Thickness Macular Hole Detection: Comparison of Missed Hole Rates and Full-Thickness Detection Indices Between Different Scan Patterns

| Scan Pattern | Comparison | Missed Hole Rate (%) | 90% CI[a] | Full-Thickness Detection Index (mean ± SD) | P[b] |
|---|---|---|---|---|---|
| 24-line radial | vs 61 raster | 0.0 | N/A | 0.66 ± 0.34 | P < .001 |
| | vs 6 radial | 0.0 | N/A | | |
| 61-line raster | vs 24 radial | 20.0 | 8.2–37.5 | 0.40 ± 0.26 | P = .751 |
| | vs 6 radial | 13.0 | 3.4–28.2 | | |
| 6-line radial | vs 24 radial | 12.0 | 3.7–30.4 | 0.65 ± 0.35 | P < .001 |
| | vs 61 raster | 4.3 | 0.2–19.0 | | |

[a]Exact (Clopper Pearson) 90% binomial confidence intervals.
[b]Exact *P* values via Wilcoxon signed rank test.

parameters between "missed" and "detected" holes using a single scan pattern/density (Wilcoxon rank sum test). Fisher exact test was used for comparisons of qualitative hole parameters in these same groups. Intergrader agreement for categorical variables was assessed via Cohen's kappa while intraclass correlation analysis was used to evaluate intergrader reliability for continuous variables. Intergrader disagreements regarding the presence or absence of a full-thickness defect were adjudicated by a third, expert grader (T.M.).

## RESULTS

A TOTAL OF 25 EYES FROM 24 PATIENTS WITH SMALL FULL-thickness macular holes underwent same-visit OCT evaluation using standard volume raster as well as 24-line radial scanning and were included in the study. The mean age (± SD) of included patients was 67.8 (± 7.3) years. The mean minimum linear diameter of included holes was 227.8 μm (± 141.4 μm) with 64% (16/25) of holes characterized as stage 2 (Gass classification).[11] A prehole opacity ("flap") (Figure 2) was present in 40% (10/25) of eyes while a persistent vitreomacular adhesion was detected in 52% (13/25).

Small full-thickness defects—which were detected with the 24-line radial scan pattern—were missed in 5 eyes (missed hole $rate_{61v24}$ = 20%; 90% confidence interval [CI] 8.2%–37.5%) and 3 eyes (missed hole $rate_{6v24}$ = 12%; 90% CI 3.7%–30.4%) with 61-line raster and 6-line radial scanning, respectively. No full-thickness defects were detected on either 61-line raster or 6-line radial scans that were missed using the 24-line radial scan protocol (missed hole $rate_{24v61}$ = 0%; missed hole $rate_{24v6}$ = 0%). Three full-thickness defects were detected on 6-line radial scans that were missed with the 61-line raster scan protocol (missed hole $rate_{61v6}$ = 13.0%, 90% CI 3.4%–28.2%), while 1 full-thickness defect was detected on the 61-line raster scans that was missed with 6-line radial scanning (missed hole $rate_{6v61}$ = 4.3%, 90% CI 0.2%–19.0%) (Table 1). Intergrader agreement was perfect for all 75 scans reviewed (intergrader agreement = 100%; kappa = 1.0).

**TABLE 2.** Impact of Optical Coherence Tomography Scan Pattern on Full-Thickness Macular Hole Detection: Comparison of Quantitative Hole Parameters Between Different Scan Patterns

| | N | Mean MLD (Mean ± SD) (Median) | P[a] | Mean BD (Mean ± SD) (Median) | P[a] | Mean MHIO (Mean ± SD) (Median) | P[a] |
|---|---|---|---|---|---|---|---|
| 61-line raster | | | | | | | |
| Missed | 5 | 91.8 ± 48.7 μm<br>86.0 μm | .002 | 298.9 ± 287.7 μm<br>180.7 μm | .015 | 66.8 ± 52.3 μm<br>60.0 μm | .019 |
| Detected | 20 | 261.8 ± 136.7 μm<br>240.7 μm | | 655.1 ± 320.5 μm<br>611.9 μm | | 207.6 ± 85.9 μm<br>199.8 μm | |
| 6-line radial | | | | | | | |
| Missed | 3 | 176.2 ± 31.6 μm<br>173.4 μm | .606 | 457.7 ± 294.9 μm<br>291.3 μm | .550 | 60.8 ± 42.7 μm<br>76.8 μm | .067 |
| Detected | 22 | 234.9 ± 147.1 μm<br>195.6 μm | | 601.0 ± 349.3 μm<br>542.0 μm | | 190.0 ± 94.8 μm<br>175.7 μm | |
| ICC | | 0.983 | – | 0.999 | – | 0.991 | – |

BD = base diameter; ICC = intraclass correlation; MHIO = macular hole inner opening; MLD = minimum linear diameter.
All full-thickness holes successfully detected on 24-line radial scanning.
[a]Exact *P* values via Wilcoxon rank sum test.

**TABLE 3.** Impact of Optical Coherence Tomography Scan Pattern on Full-Thickness Macular Hole Detection: Comparison of Qualitative Hole Parameters Between Different Scan Patterns

| | N | Prehole Flap | P[a] | VMA | P[a] | VPA | P[a] | ERM | P[a] |
|---|---|---|---|---|---|---|---|---|---|
| 61-line raster | | | | | | | | | |
| Missed | 5 | 4/5 | .121 | 4/5 | .322 | 4/5 | 1.00 | 2/5 | .597 |
| Detected | 20 | 6/20 | | 9/20 | | 16/20 | | 5/20 | |
| 6-line radial | | | | | | | | | |
| Missed | 3 | 3/3 | .052 | 3/3 | .220 | 3/3 | 1.00 | 1/3 | 1.00 |
| Detected | 22 | 7/22 | | 10/22 | | 15/20 | | 6/20 | |

ERM = epiretinal membrane; VMA = vitreomacular adhesion; VPA = vitreopapillary adhesion.
All full-thickness holes successfully detected on 24-line radial scanning.
[a]*P* values via Fisher exact test.

The Supplemental Video (available at AJO.com) depicts the individual raster and radial B-scans from an eye in which a hole was missed on standard raster volume scanning but detected on 24-line radial scanning.

The proportion of B-scans within an individual study depicting a full-thickness hole was significantly greater when using the 24-line radial (full-thickness detection index = 0.66 ± 0.34, $P < .001$) and 6-line radial (full-thickness detection index = 0.65 ± 0.35, $P < .001$) as compared to 61-line raster scanning (full-thickness detection index = 0.40 ± 0.26). The full-thickness detection indices were similar for the 2 radial scan patterns tested ($P = .751$). A full-thickness defect was detected in a mean of 15.1 ± 8.8 scans (range 2-24) using the 24-line radial pattern and a mean of 3.8 ± 2.2 scans (range 1–6) using the 6-line radial pattern.

For any single MH, the largest minimum linear hole diameter detected with 24-line scanning was significantly greater than the corresponding value detected by the 6-line radial ($P < .001$) and 61-line raster ($P = .023$) scan patterns. Similarly, the smallest minimum linear hole diameter detected with the 24-line radial scan pattern was significantly less than that detected with the 6-line radial pattern ($P < .001$). No difference in the smallest minimum linear hole diameter was found when comparing radial to raster scanning ($P = .418$ for 24-line radial vs 61-line raster; $P = .734$ for 6-line radial vs 61-line raster).

In general, full-thickness holes missed on 61-line raster scanning but detected on 24-line radial scans were smaller and more commonly associated with a persistent vitreomacular adhesion (VMA) and a prehole flap. Based on manually measured values from the 24-line radial scan, mean minimum hole diameter ($P = .002$), mean hole base diameter ($P = .015$), and mean macular hole inner opening ($P = .019$) were all significantly smaller in eyes in which a full-thickness hole was missed with the raster scan protocol. Prehole flaps were found in 4 of 5 missed holes as compared to 6 of 20 detected holes, while persistent VMA was present in 4 of 5 missed holes as compared to 9 of 20 detected holes; however, neither of these comparisons reached statistical significance ($P = .121$ for prehole flap; $P = .322$ for VMA) (Table 2, Table 3).

Holes missed on 6-line radial scans but detected with the 24-line radial pattern were not significantly smaller than holes detected with both scan patterns, though there was a trend toward smaller mean macular hole inner openings

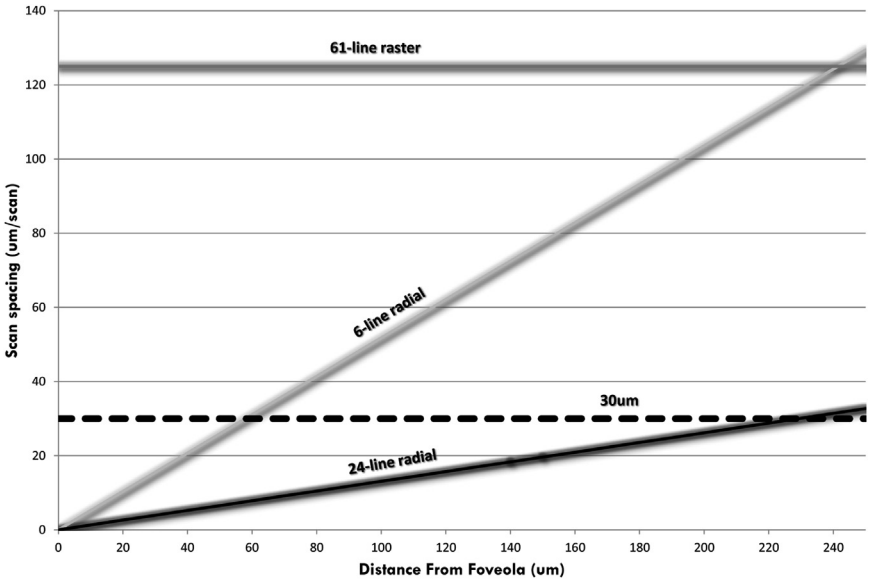


**FIGURE 3. Relationship between interscan spacing and distance of a representative B-scan from the foveola. The dashed line at 30 μm signifies the smallest interscan spacing currently attainable using factory default volume raster scan patterns on commercially available Spectralis and Zeiss optical coherence tomography units (eg, "Detail" scan pattern on the Heidelberg Spectralis unit and the "200 × 200 Macular Cube" on the Zeiss Cirrus unit).**

in the missed holes ($P = .067$). Similarly, no significant associations were found between any qualitative parameters assessed and the failure to detect a full-thickness defect on 6-line radial scanning; however, a trend toward greater prevalence of prehole flaps ($P = .052$) was seen when comparing missed to detected holes (Table 2, Table 3).

Of note, intergrader reliability was excellent for manually measured hole parameters with intraclass correlation >0.98 for all 3 quantitative parameters evaluated (Table 2).

## DISCUSSION

THE AIM OF THIS STUDY WAS TO EVALUATE THE IMPACT OF different OCT scan patterns and scan densities on the diagnosis of small full-thickness macular holes. Our results suggest that radial scan patterns, particularly with a high density of B-scans, may be superior to standard raster volume scans used routinely for evaluation of macular thickness in diseases such as neovascular AMD and DME. Specifically, the use of a standard raster volume scan protocol was associated with a clinically unacceptable rate of missed holes (20%, 90% CI 8.2%–37.5%), which were detected on a custom 24-line radial scan pattern acquired at the same visit. A smaller but likely still clinically relevant rate of missed holes (12%, 90% CI 3.7%–30.4%) occurred when using a lower radial density (6 lines vs 24 lines). This would suggest that in order to maximize the sensitivity of OCT-based full-thickness MH detection, a radial scan pattern should be routinely employed in patients with suspected holes. Furthermore, increasing the radial scan density above the historic 6-line standard—which has been employed in numerous major studies of idiopathic macular hole[12–14]—may also further enhance detection. Not surprisingly, holes missed on raster volume scanning but detected with the high-density radial scan protocol were significantly smaller, with a trend toward a greater prevalence of prehole flaps as well as persistent VMAs. Further reinforcing the notion that radial scanning may be superior for the evaluation of full-thickness MHs, a significantly greater proportion of B-scans included in the radial scan protocol depicted a full-thickness defect when compared to the raster scan pattern. High-density radial scanning also appeared to more accurately reflect hole dimensions as the largest minimum linear hole diameter detected by the 24-line scan pattern was greater than the corresponding value found with either 6-line radial or 61-line raster scanning. This finding likely reflects the irregular nature of full-thickness macular defects, which results in widely differing hole diameters depending on the angle of measurement relative to the horizontal raphe. Such differences may be clinically relevant as the greatest linear hole dimension determines hole staging and prognosis for closure, and is a common inclusion/exclusion criterion in clinical studies.

To date, there is a dearth of data regarding the relative utility of different OCT scan patterns and densities in the detection of full-thickness MHs. One group has examined the impact of varying OCT scan density in the detection/measurement of important parameters in neovascular

AMD[9] and DME[10] and shown only a modest effect on the sensitivity/accuracy of the attendant results. However, both neovascular AMD and DME are pan-macular diseases with OCT findings that routinely extend well beyond the fovea and are notably less focal than those associated with idiopathic macular hole. Perhaps more relevant to this study is a recent post hoc analysis comparing results from time-domain OCT (TD OCT) to those from spectral-domain OCT (SD OCT) in the large clinical trial evaluating the efficacy of ocriplasmin in the treatment of symptomatic VMA (including small full-thickness MHs). In this analysis, out of 173 eyes examined, 4 baseline full-thickness MHs were detected on TD OCT but missed on SD OCT, while only a single full-thickness MH was seen on SD OCT that was missed on TD OCT.[15] This finding is highly surprising in light of the well-documented superior resolution of SD OCT, but can likely be explained by differences in scan patterns—the TD OCT equipment employed 6-line radial scan protocols while the SD OCT machines used raster volume scanning. These findings raise the possibility that routine use of high-density radial OCT scan patterns may afford earlier detection of full-thickness MHs, which may in turn lead to earlier treatment and the prevention of vision loss associated with more advanced-stage macular holes.

In addition to a potential negative impact on clinical outcomes, failure to detect such early full-thickness holes may confound clinical trials examining therapeutic outcomes for patients with vitreoretinal interface disease (eg, symptomatic vitreomacular adhesion, vitreomacular traction syndrome, and macular hole). As these trials now routinely employ OCT as the defining inclusion criteria, missed holes will lead to misclassification with the possibility of erroneously poor outcomes.

This issue will become increasingly important as the recent approval of ocriplasmin (Jetrea; Thrombogenics, Inc, Iselin, New Jersey, USA) will undoubtedly spur further investigations into novel pharmacologic vitreolytic agents.

We postulate that the superior detection of full-thickness MHs seen with high-density radial scanning when compared to standard raster volume scanning results from 2 factors: (1) greater foveolar scan density; and (2) better approximation of macular hole geometry. As seen in Figure 3, the B-scan spacing achieved with the 24-line radial scan is dramatically smaller at clinically relevant distances from the foveola when compared to both standard raster volume scanning as well as lower-density radial scanning. In theory, the foveolar/perifoveolar scan spacing attained with 24-line radial scanning may prove to be superior to even the 30 μm spacing achieved with default raster scan modes dedicated to high-density macular analysis (eg, the "Detail" scan seen on the Heidelberg Spectralis and the 200 × 200 macular cube seen on the Zeiss Cirrus) (Figure 3). As the pathologic changes associated with the idiopathic macular holes are concentrated in the foveolar/perifoveolar region, density of B-scans at the foveola is of the utmost importance in maximizing detection of small full-thickness defects. It should be noted that patients with full-thickness MHs have been shown to preferentially fixate not at the foveolar center, but rather at the margin of the full-thickness neurosensory defect (located at a distance equivalent to one-half the minimum linear hole diameter from the foveolar center).[16,17] This may lead to decentration of the radial scan away from the foveolar center; this, however, can be addressed by manually recentering scans on to the foveola during acquisition if eccentric fixation is detected, as it was done in this study. As seen in the Supplemental Video, excellent radial scan centration was obtained despite the presence of a full-thickness defect.

As an additional benefit, greater scan density is achieved with many fewer B-scans than required in standard raster volume scans, which should allow for greater ease of acquisition and potentially fewer scan artifacts from patient movement. Additionally, the radial scan pattern better follows the typically round geometry of pathogenic VMA/macular holes, making it more likely to detect an early eccentric full-thickness hole.

We acknowledge several limitations of our study. Chief among those is the retrospective design and small sample size, which was a result of the finite number of suspected small holes that were flagged for concurrent radial and raster scanning. Furthermore, the inclusion of only suspected small full-thickness MHs for concurrent scanning undoubtedly induced some degree of selection bias; thus, it is likely that the actual missed hole rate is lower than reported here if considering full-thickness MHs of all sizes. As patients in this study were imaged exclusively with the Heidelberg Spectralis OCT unit, it may limit the generalizability of these findings to other OCT machines. In the future, design of prospective studies using greater raster and radial scan density may allow for a receiver operating characteristic analysis to identify the optimal custom scan protocol for macular hole detection.

In summary, we present a novel analysis demonstrating superior performance of high-density radial OCT scan protocols in the detection small full-thickness MHs. Though this is a small study, it highlights the importance of OCT scan pattern selection in maximizing the sensitivity of detection of macular pathology. It will be imperative for future investigators to consider these results in designing imaging protocols for large-scale clinical trials focused on treatment of full-thickness MHs. Additionally, manufacturers of OCT equipment should take note of the important role of radial scanning in the evaluation of foveolar pathology as many machines do not currently support true radial scanning.

ALL AUTHORS HAVE COMPLETED AND SUBMITTED THE ICMJE FORM FOR DISCLOSURE OF POTENTIAL CONFLICTS OF INTEREST. Dr Tamer Mahmoud reported participation in an advisory board for Alimera (Alpharetta, Georgia). No other disclosures were reported. No financial support was provided for this study. All authors contributed substantially to the conduct of this research as follows: design and conduct of study (E.S., B.T., M.K., T.M.); collection of data (E.S., B.T., M.K.); management, analysis, and interpretation of data (E.S., B.T., T.M.); and preparation, review, and approval of manuscript (E.S., B.T., M.K., T.M.). Statistical consultation was kindly provided by Sandra Stinnett, Assistant Professor of Biostatistics and Bioinformatics, Duke University School of Medicine, Durham, North Carolina.

## REFERENCES

1. Tadayoni R, Gaudric A, Haouchine B, Massin P. Relationship between macular hole size and the potential benefit of internal limiting membrane peeling. *Br J Ophthalmol* 2006; 90(10):1239–1241.
2. Lanzetta P, Polito A, Del Borrello M, et al. Idiopathic macular hole surgery with low-concentration infracyanine green-assisted peeling of the internal limiting membrane. *Am J Ophthalmol* 2006;142(5):771–776.
3. Nomoto H, Shiraga F, Yamaji H, et al. Macular hole surgery with triamcinolone acetonide-assisted internal limiting membrane peeling: one-year results. *Retina* 2008;28(3):427–432.
4. Tognetto D, Grandin R, Sanguinetti G, et al. Internal limiting membrane removal during macular hole surgery: results of a multicenter retrospective study. *Ophthalmology* 2006;113(8):1401–1410.
5. Jaycock PD, Bunce C, Xing W, et al. Outcomes of macular hole surgery: implications for surgical management and clinical governance. *Eye (Lond)* 2005;19(8):879–884.
6. Ullrich S, Haritoglou C, Gass C, Schaumberger M, Ulbig MW, Kampik A. Macular hole size as a prognostic factor in macular hole surgery. *Br J Ophthalmol* 2002;86(4): 390–393.
7. Kim JW, Freeman WR, Azen SP, el-Haig W, Klein DJ, Bailey IL. Prospective randomized trial of vitrectomy or observation for stage 2 macular holes. Vitrectomy for Macular Hole Study Group. *Am J Ophthalmol* 1996;121(6):605–614.
8. Azzolini C, Patelli F, Brancato R. Correlation between optical coherence tomography data and biomicroscopic interpretation of idiopathic macular hole. *Am J Ophthalmol* 2001; 132(3):348–355.
9. Baranano AE, Keane PA, Ruiz-Garcia H, Walsh AC, Sadda SR. Impact of scanning density on spectral domain optical coherence tomography assessments in neovascular age-related macular degeneration. *Acta Ophthalmol* 2012; 90(4):e274–e280.
10. Nittala MG, Konduru R, Ruiz-Garcia H, Sadda SR. Effect of OCT volume scan density on thickness measurements in diabetic macular edema. *Eye (Lond)* 2011;25(10):1347–1355.
11. Gass JD. Reappraisal of biomicroscopic classification of stages of development of a macular hole. *Am J Ophthalmol* 1995; 119(6):752–759.
12. Ip MS, Baker BJ, Duker JS, et al. Anatomical outcomes of surgery for idiopathic macular hole as determined by optical coherence tomography. *Arch Ophthalmol* 2002;120(1):29–35.
13. Haouchine B, Massin P, Tadayoni R, Erginay A, Gaudric A. Diagnosis of macular pseudoholes and lamellar macular holes by optical coherence tomography. *Am J Ophthalmol* 2004; 138(5):732–739.
14. Stalmans P, Benz MS, Gandorfer A, et al. Enzymatic vitreolysis with ocriplasmin for vitreomacular traction and macular holes. *N Engl J Med* 2012;367(7):606–615.
15. Folgar FA, Toth CA, DeCroos FC, Girach A, Pakola S, Jaffe GJ. Assessment of retinal morphology with spectral and time domain OCT in the phase III trials of enzymatic vitreolysis. *Invest Ophthalmol Vis Sci* 2012;53(11):7395–7401.
16. Guez JE, Le Gargasson JF, Massin P, Rigaudiere F, Grall Y, Gaudric A. Functional assessment of macular hole surgery by scanning laser ophthalmoscopy. *Ophthalmology* 1998; 105(4):694–699.
17. Nakabayashi M, Fujikado T, Ohji M, Saito Y, Tano Y. Fixation patterns of idiopathic macular holes after vitreous surgery. *Retina* 2000;20(2):170–175.

## Biosketch

Eric W. Schneider, MD is completing a fellowship in vitreoretinal surgery at the Duke University Eye Center. He obtained a Bachelor of the Arts degree from Brown University. He completed both his medical school and residency training at the University of Michigan. Dr Schneider's research interests include vitreoretinal interface disorders, retinal vascular disease, ocular immunology, and novel applications of retinal imaging. Following completion of fellowship in June 2014, he will be joining Tennessee Retina in Nashville, TN.